# State diagrams for harmonically trapped bosons in optical lattices

Marcos Rigol

*Department of Physics, Georgetown University, Washington, DC 20057, USA*

George G. Batrouni

*INLN, Université de Nice-Sophia Antipolis, CNRS; 1361 route des Lucioles, 06560 Valbonne, France*

Valery G. Rousseau

*Instituut-Lorentz, LION, Universiteit Leiden, Postbus 9504, 2300 RA Leiden, The Netherlands*

Richard T. Scalettar

*Department of Physics, University of California, Davis, California 95616, USA*

We use quantum Monte Carlo simulations to obtain zero-temperature state diagrams for strongly correlated lattice bosons in one and two dimensions under the influence of a harmonic confining potential. Since harmonic traps generate a coexistence of superfluid and Mott insulating domains, we use local quantities such as the quantum fluctuations of the density and a local compressibility to identify the phases present in the inhomogeneous density profiles. We emphasize the use of the "characteristic density" to produce a state diagram that is relevant to experimental optical lattice systems, regardless of the number of bosons or trap curvature and of the validity of the local-density approximation. We show that the critical value of $U/t$ at which Mott insulating domains appear in the trap depends on the filling in the system, and it is in general greater than the value in the homogeneous system. Recent experimental results by Spielman *et al.* [Phys. Rev. Lett. **100**, 120402 (2008)] are analyzed in the context of our two-dimensional state diagram, and shown to exhibit a value for the critical point in good agreement with simulations. We also study the effects of finite, but low ($T \leq t/2$), temperatures. We find that in two dimensions they have little influence on our zero-temperature results, while their effect is more pronounced in one dimension.

## I. INTRODUCTION

A great amount of experimental and theoretical work [1] has followed the successful realization of the superfluid(SF)-to-Mott-insulator transition in ultracold bosonic gases trapped in optical lattices, in three [2], two [3], and one [4] dimensions. Ultracold atoms on optical lattices are envisioned as ideal analog simulators of Hamiltonians such as the fermion Hubbard model, which so far suffers from the lack of reliable analytical and numerical results. As a first step toward this goal, intensive efforts are currently under way to validate this approach by comparing experimental and theoretical results for systems such as the Bose-Hubbard model that are amenable to both treatments. However, even this is challenging, since the phase diagram of the Bose-Hubbard model is complicated by issues such as spatial inhomogeneities (recognized early in Refs. [5, 6]), finite-temperature effects [7, 8, 9, 10], and the limited set of experimental tools available to characterize those systems.

The phase diagram of the homogeneous Bose-Hubbard model is known to consist of (i) superfluid phases for all incommensurate fillings and arbitrary values of the ratio between the on-site repulsion and the hopping parameter $(U/t)$. The system is also superfluid for commensurate fillings when $U/t$ is smaller than some critical value $(U/t)_c$, which depends on the dimensionality of the system and on the (integer) filling. (ii) Mott insulat-

ing phases are present for commensurate fillings when $U/t > (U/t)_c$ [11, 12, 13, 14, 15]. These two phases have been shown to coexist when a confining potential is added to the model [5, 6, 16, 17, 18]. A feature in the trap, which is advantageous from the experimental point of view, is that in inhomogeneous systems Mott insulating domains appear for a broad range of fillings, as opposed to the few commensurate fillings required for the translationally invariant system. This feature comes at a price, sometimes ignored for the sake of simplicity by both experimentalists and theoreticians working on these systems. In trapped lattice bosons the critical value $(U/t)_c^T$ for the formation of Mott insulating domains in different places in the trap not only depends on the local filling and the dimensionality of the system (the case for homogeneous systems) but also on the total filling $N$ in the trap and the curvature of the confining potential $V$. A useful, but approximate, understanding of the effect of confinement, which we will not employ here, can be obtained through the use of the local-density approximation (LDA).

One may think that having to deal with different fillings and trapping potential parameters in different experiments makes the determination of a state diagram [19] in one particular experimental setup not relevant to any other. This is not the case. In Refs. [20, 21], it was shown by means of quantum Monte Carlo (QMC) simulations that for lattice fermions in one dimension one can

define a scaled dimensionless variable, the characteristic density $\tilde{\rho} = Na(V/t)^{1/2}$ (where $a$ is the lattice spacing), which allows one to build a state diagram in the plane $\tilde{\rho}$ vs $U/t$ that is insensitive to the individual values of $N$ and $V$ [22]. The form for $\tilde{\rho}$ can most simply be understood as arising from dimensional arguments: the trap curvature $V$ has units of energy/length$^2$, so that $(V/t)^{1/2}$ has units of inverse length. One can then define a length scale $\xi = (V/t)^{-1/2}$, which for trapped systems plays a role similar to the system size $L$ in the homogeneous case. The characteristic density $\tilde{\rho} = N_b a/\xi$ is then a dimensionless quantity, which for trapped systems is the analog of the filling per site $n = N_b a/L$ in the homogeneous case. In other words, $\tilde{\rho}$ defines how one should approach the thermodynamic limit in trapped systems.

The characteristic density is not only relevant to one-dimensional systems. It can be generalized to higher dimensions $d$, $\tilde{\rho} = Na^d(V/t)^{d/2}$ [27, 28]. In recent work, the state diagram of the three-dimensional Fermi-Hubbard model in a harmonic trap was obtained by using a combination of dynamical mean-field theory (a treatment which ignores the momentum dependence of the self-energy while retaining its time fluctuations) and the LDA [29].

One may construct the state diagram in a trap using results for the homogeneous system combined with the LDA. However, this approach is only approximate for finite systems. While LDA has been shown to give reasonably accurate results in many regimes under a confining potential, it is certainly bound to fail close to the critical values of $U/t$ at which Mott insulating domains are formed. This is because in the homogeneous system, there are diverging correlations when one crosses the quantum critical region, i.e., finite-size effects in the trap not only become relevant but are also unavoidable. We will show in this paper that in those regimes where LDA fails, our exact QMC-based state diagram is an accurate tool for characterization of the experimental results.

Since state diagrams are not available for lattice bosons, in this paper we use world-line quantum Monte Carlo simulations to generate the zero-temperature state diagram for the one- and two-dimensional (2D) Bose-Hubbard model under the influence of a harmonic confining potential. The state diagram in two dimensions allows us to analyze recent experimental results for confined two-dimensional bosons in optical lattices [3] without the need to perform simulations for the same parameters as in the experiments. We find that the critical values for the formation of Mott insulating domains reported in Ref. [3] are consistent (within experimental errors) with our theoretical results for inhomogeneous systems. Finally, we will discuss the effect that a small increase in the temperature ($T \leq t/2$) has on our ground-state results. The latter is found to have little consequence in two dimensions, where the $U/t$ values which demark the boundaries between states only change by a few percent.

In one dimension, we find that the trapping potential has an even stronger influence on the critical values of $U/t$ at which Mott insulating domains appear in the trap. We will also show that low temperatures have a pronounced effect on the inhomogeneous states in the trap. The important issue of how to detect experimentally the different phases in the trap is addressed in several recent works (see, *e.g.*, [17, 18, 29, 30, 31, 32, 33, 34, 35, 36]) and will not be discussed here.

## II.  TRAPPED BOSONS IN TWO DIMENSIONS

### A.  Hamiltonian and local observables

For deep enough optical lattices and low temperatures, confined bosons in two dimensions can be described by the Bose-Hubbard Hamiltonian [16]

$$
\begin{aligned}
H = {} & -t \sum_{\langle i,j \rangle} \left( a_i^\dagger a_j + \text{H.c.} \right) + \frac{U}{2} \sum_i n_i \left( n_i - 1 \right) \\
& + V \sum_i r_i^2 \, n_i \ .
\end{aligned}
\tag{1}
$$

Here $a_i^\dagger$ and $a_i$ are the creation and annihilation operators of a boson at site $i$, located at a distance $r_i = \sqrt{x_i^2 + y_i^2}$ from the center of the trap. $x_i$ and $y_i$ are given in units of the lattice spacing, set to unity in this work. $n_i = a_i^\dagger a_i$ is the particle number operator. The on-site interaction parameter is denoted by $U$ ($U > 0$), the nearest-neighbor hopping amplitude is denoted by $t$, and $V$ is the curvature of the harmonic confining potential. In experiments on optical lattices, $t$, $U$, and $V$ can be controlled by changing the intensity of the laser beams that produce the lattice. One can also control $U$ separately using Feshbach resonances [1]. We performed QMC simulations in the canonical ensemble, using the world-line algorithm [37]. For our-zero temperature study, we have taken the inverse temperature to be $\beta t = 18$, which is sufficient to obtain ground-state results for the observables considered here (see discussion in Fig. 3), and for discretizing imaginary time we have chosen $t \Delta\tau = 0.1$.

In order to create the state diagram, we will monitor three local observables. The first one is the density. Plateaus with constant integer density are the so-called Mott insulating domains [5]. However, since the local density always crosses integer fillings as the total number of bosons in the trap is increased, and since close to integer local fillings and for large enough values of $U/t$ one always sees some kind of shoulder appearing in the density profiles (see, *e.g.*, Figs. 1 and 3), identifying the formation of Mott domains only by means of the density is not accurate [20, 21].

The second local quantity we monitor is the quantum fluctuations of the density, also referred to as the variance of the density,

$$
\Delta_i = \langle n_i^2 \rangle - \langle n_i \rangle^2 .
\tag{2}
$$

As shown in Refs. [20, 21], this quantity exhibits a local minimum for densities closest to integer fillings. In addition, once a Mott insulating domain forms, the value at the minimum equals the value of the variance in the Mott insulating phase of an equivalent homogeneous system, i.e., a translationally invariant system with exactly the same density and $U/t$ [20, 21]. We will show here that in our finite lattice-boson systems (such as the ones created experimentally), shoulders with $n \simeq 1$ can appear without the variance of the density on those shoulders attaining the value in the homogeneous Mott insulator. That is, those shoulders are not local Mott insulating domains.

The final quantity that we measure here is the local compressibility defined in Refs. [5, 18],

$$\kappa_i = \frac{\partial n_i}{\partial \mu_i} = \frac{1}{\beta} \left[ \left\langle \left( \int_0^\beta d\tau n_i(\tau) \right)^2 \right\rangle - \left\langle \int_0^\beta d\tau n_i(\tau) \right\rangle^2 \right]. \tag{3}$$

This local compressibility quantifies the response in the on-site density to a local change of the chemical potential. $\kappa_i$ also exhibits a minimum around integer fillings, and it behaves, qualitatively, similarly to $\Delta_i$. An analogous distinction between equal-time fluctuations and susceptibilities which include unequal-time correlations plays an important role in the fermion Hubbard model, where the local susceptibility carries additional information about the (Kondo) screening beyond that contained in the equal-time local moment.

### B. Density, variance, and local compressibility

In Fig. 1, we show two density profiles in a two-dimensional harmonic trap for values of the on-site repulsive interaction right before ($U/t = 17.5$) and right after ($U/t = 18.5$) the formation of the Mott insulator in the middle of the trap. For $U/t = 17.5$ [Fig. 1(a)], one can see that a shoulder with density $n \sim 1$ has developed in the system, but the density in the center of the trap is slightly greater than 1. For $U/t = 18.5$ [Fig. 1(b)] only a plateau with density $n = 1$ is seen at the central region of the system. Positions in the trap are normalized by a length scale $\xi = \sqrt{t/V}$, which is introduced in Hamiltonian (1) by the harmonic confining potential. With this normalization, systems with different trapping potentials and fillings, but with the same characteristic density, have identical density profiles [20, 21, 28].

Intensity plots of the variance and local compressibility profiles corresponding to the systems in Fig. 1 are presented in Fig. 2. This figure shows that both $\Delta$ and $\kappa$ exhibit minima whenever the density is closest or equal to 1. In addition, in Figs. 2(a) and 2(b) one can see that the region with $n > 1$ at the center of the trap in Fig. 1(a) is signaled by local maxima of $\Delta$ and $\kappa$.

A more quantitative understanding of the behaviors of $n$, $\Delta$, and $\kappa$ can be gained by plotting the changes in
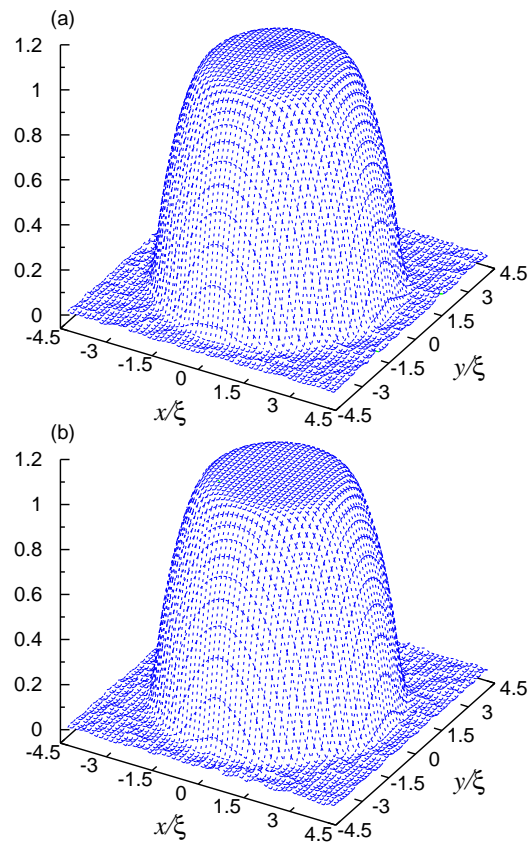


FIG. 1: (Color online) Two-dimensional density profiles for systems with $\tilde{\rho} = 30$ ($N_b = 1200$ and $V/t = 0.025$), $\beta = 18$, $L_x = L_y = 60$ (number of lattice sites along $x$ and $y$), and in-site repulsion (a) $U/t = 17.5$ and (b) $U/t = 18.5$. Positions in the trap are normalized by the length scale $\xi = \sqrt{t/V}$ (see text). For the homogeneous model (V/t=0) the critical value $(U/t)_c$ for the SF-Mott transition in $d = 2$ is 16.74 [15].

these quantities along one spatial dimension, while the coordinate in the other spatial dimension is fixed to the center of the trap. The results for the systems in Figs. 1 and 2 are shown in Fig. 3, which confirms that, indeed, minima of $\Delta$ and $\kappa$ correspond to regions with $n \simeq 1$ in the density profiles. Along with the results in the trap, we have plotted as horizontal lines the values of the density, variance, and compressibility in the Mott insulating phase of the homogeneous system for exactly the same values of $U/t$.

Figures 3(a)–(c) ($U/t = 17.5$) show an important property of these finite trapped systems. While the density profile can exhibit a shoulder with $n \simeq 1$ [Fig. 3(a)] when crossing $n = 1$, the variance and local compressibilities on this shoulder do not reach their values in the first lobe of homogeneous systems, for exactly the same values of $U/t$. The LDA is not valid in this region of the trap. Notice that in Figs. 3(a)–3(c) such a shoulder is present for a value of $U/t$ that is greater than the critical value $(U/t)_c$ for the formation of the Mott insulator in the homogeneous system, which is $(U/t)_c = 16.74$ for $n = 1$ in two dimensions [15]. Therefore, *no* local Mott insulating
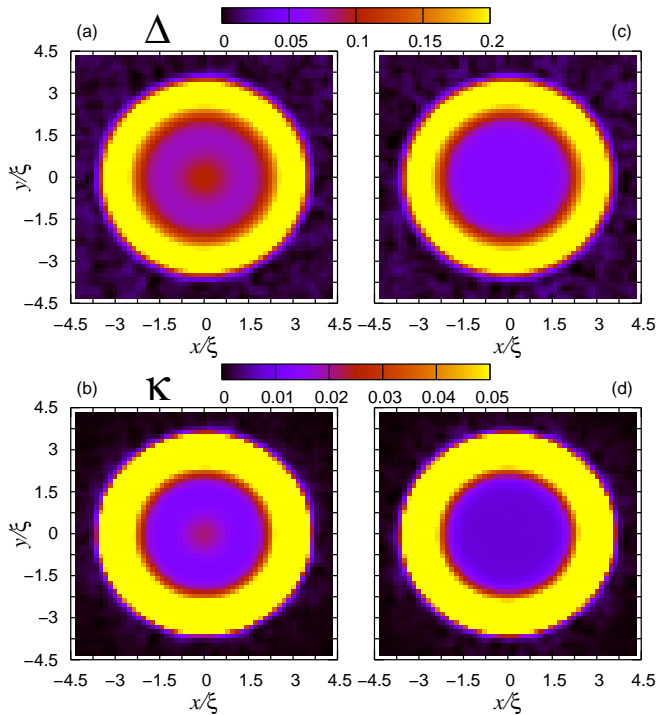
FIG. 2: (Color online) Intensity plots of the local quantum fluctuations of the [(a) and (c)] density $\Delta$ and [(b) and(d)] local compressibility $\kappa$ for [(a) and (b)] $U/t = 17.5$ and [(c) and (d)] $U/t = 18.5$. In these systems $\tilde{\rho} = 30$ ($N_b = 1200$ and $V/t = 0.025$), $\beta = 18$, and $L_x = L_y = 60$. The corresponding density profiles are plotted in Fig. 1.
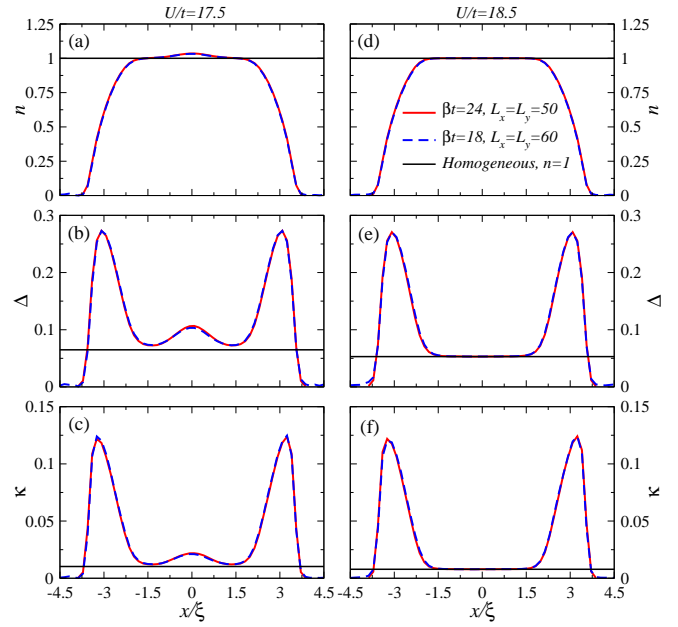


FIG. 3: (Color online) Cuts across the center of the trap for the two-dimensional density, variance, and local compressibility plots in Figs. 1 and 2 [$\tilde{\rho} = 30$ ($N_b = 1200$ and $V/t = 0.025$), $\beta = 18$, and $L_x = L_y = 60$]. Horizontal lines show the results in homogeneous systems for the same values of $U/t$, $\beta$, and $n = 1$. These results emphasize that the LDA does not hold in some regions of the trap. In the $n \sim 1$ domains in panel (a) that develop around commensurate filling, the variance in panel (b) does not take on the value predicted by the homogeneous system for $n = 1$. We also plot results for a smaller system with $L_x = L_y = 50$, at lower temperature $\beta = 24$, and the same value of $\tilde{\rho} = 30$ ($N_b = 1200$ and $V/t = 0.025$).

phase is found in a trap *for $U/t > (U/t)_c$* and the density at the center of the trap is $n \geq 1$. In an experiment with bosons trapped in optical lattices, the critical value for the formation of a Mott insulating state may be greater than the critical value in homogeneous systems. This is due to the finite curvature of the trapping potential and the finite (and sometimes small) extent of the system. How much the critical value is shifted from the homogeneous prediction is something that, as we will show later, will strongly depend on the dimensionality of the system.

In Figs. 3(d)–3(f) one can see that for $U/t = 18.5$ a full region with $n = 1$ occupies the center of the trap. In that region, $\Delta$ and $\kappa$ have exactly the same values as that in the homogeneous system with $n = 1$ for an identical on-site repulsion $U/t$. Hence, we conclude that the domain in the middle of the trap is in this case a Mott insulator.

To conclude this subsection on local observables, we discuss whether the lattice size considered in Figs. 1 and 2 is big enough so that *boundary conditions* are irrelevant, and whether the temperature is low enough so that $n$, $\Delta$, and $\kappa$ behave as they will in the ground state. In Fig. 3, we present results for a system with identical Hamiltonian parameters and filling but at a lower temperature $\beta = 24$ and in a smaller lattice with $L_x = L_y = 50$ sites in each direction. They can be seen to be essentially indistinguishable from those with $\beta = 18$ and $L_x = L_y = 60$. Hence, at least for our local observables, the tempera-

ture considered is low enough and the systems sizes are big enough so that they have no influence in our results.

## C.   State diagram

Uniform systems of different sizes have identical properties as long as they are chosen to have the same density $\rho = N_b/L^d$, or in a lattice the same $n = N_b a^d/L^d$, and are sufficiently large. In a similar way, the characteristic density generalizes this for confined systems and allows one to obtain state diagrams that are independent of particular choices of boson number and trap curvature provided the systems are also large. Finite systems, such as the ones realized experimentally, pose an additional complication as finite-size effects become relevant. They are most important close to where local phases (such as those described in Sec. II B) appear for the first time in the trap. This implies that, as also shown in Sec. II B, the LDA may fail to describe the actual density profiles in an ultracold gas experiment on an optical lattice.

In this section we show that, for systems like the ones realized experimentally, a state diagram in the plane $\tilde{\rho}$ vs $U/t$ can accurately predict the local phases in trapped

experiments even when the LDA fails. What this means is that for those system sizes (where the occupied part of the lattice has $50 \lesssim L_x, L_y \lesssim 100$), changing the specific trap parameters does not appreciably change the observed local phases under the confining potential. In order to create such a state diagram, we have considered systems with two different values of the trap curvature and many different fillings. We fixed the inverse temperature to $\beta = 18$ and the largest lattices considered here had $L_x = L_y = 64$ lattice sites. The lattice sizes considered here are comparable to the ones realized experimentally [3].

In the left panels of Fig. 4[(a)–(c)], we compare two systems with the same characteristic density $\tilde{\rho} = 20$, but two different trapping potentials and fillings [$N_b = 800$, $V/t = 0.025$ and $N_b = 500$, $V/t = 0.04$]. Our results for the scaled density, variance, and local compressibility profiles are essentially indistinguishable between those two traps, despite the large difference in particle number and curvature. In Figs. 4(a)–4(c), we have chosen one of the lowest characteristic densities that support a Mott insulating state in the trap. With increasing $\tilde{\rho}$, at the same values of $V/t$, the differences between the scaled profiles in the two traps become even smaller.

In the right panels of Fig. 4[(d)–(f)], we compare two systems in which an additional superfluid phase with

$n > 1$ is present inside a Mott insulating domain with $n = 1$. This state has a richer structure than the one in the left panel. The characteristic density is the same in both systems, $\tilde{\rho} = 35$, but the trap curvature and fillings are different ($N_b = 1400$, $V/t = 0.025$ and $N_b = 875$, $V/t = 0.04$). We have chosen the ratio of $U/t$ in this case to be very close to the critical value for the formation of the Mott insulator at the center of the trap. Figures 4(d)–4(f) show that even in this more complicated case, with several different domains and close to a transition between states, the scaled results for our local observables are also almost indiscernible even for two very different systems, as long as they have the same characteristic density.

In Figs. 3(a)–3(c), we have shown results for local quantities in a system that cannot be described within the LDA. In Fig. 5, we provide an additional example where two different confined systems with $U/t > (U/t)_c$ [$(U/t)_c$ from the homogeneous case] fail to exhibit Mott insulating domains. This figure also shows that even though the LDA is clearly not applicable to those systems, the density profiles and local compressibilities in both of them, which have the same characteristic density, are almost indistinguishable. As in previous figures, the number of particles in the largest system is almost twice that of the smallest. These results confirm that the characteristic density, being the proper quantity to define the thermodynamic limit in a trapped system, provides genuine guidance for finite systems when the LDA is not valid.

Following the discussion in Sec. II B), we locate Mott insulating domains in the trap by comparing the variance of the density and local compressibilities in the confined system with those of a Mott insulator in the homogeneous case. Whenever they coincide, we conclude that a local Mott insulating domain is present. With this criterion, in most cases Mott insulating domains emerge in the trap for the same value of $U/t$ independent of whether one considers $\Delta$ or $\kappa$. In a few cases, especially at low fillings, we found $\Delta$ in the trap to agree with the value in the
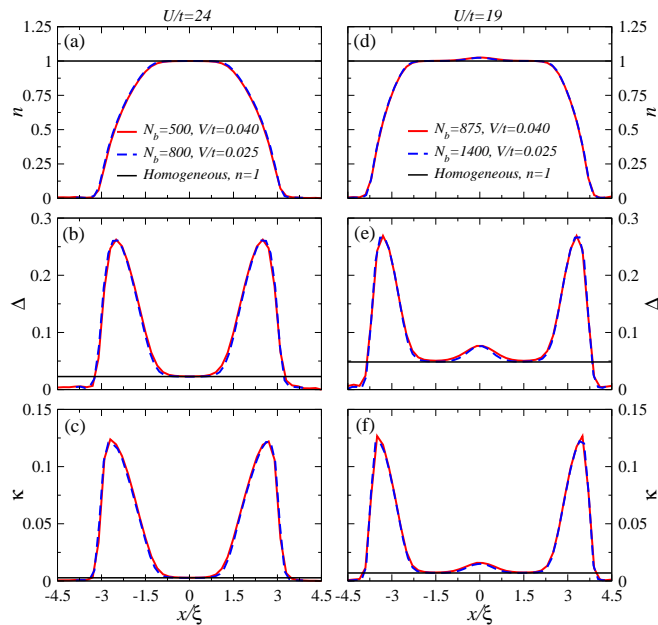


FIG. 4: (Color online) Density, variance, and local compressibility in one direction across the center of the trap. We compare systems with the same characteristic density but different trapping potentials and fillings. Left panels [(a)–(c)]: $U/t = 24$, $\tilde{\rho} = 20$, with $N_b = 800$, $V/t = 0.025$ and $N_b = 500$, $V/t = 0.04$. Right panels [(d)–(f)]: $U/t = 19$, $\tilde{\rho} = 35$, with $N_b = 1400$, $V/t = 0.025$ and $N_b = 875$, $V/t = 0.04$. In all cases $\beta = 18$. Horizontal lines show the results for homogeneous systems with $n = 1$ and the same values of $U/t$ and $\beta$ as in the trap.
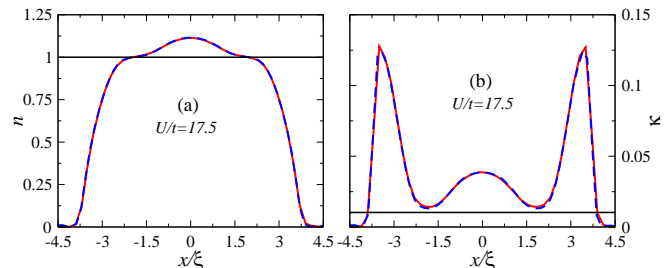


FIG. 5: (Color online) (a) Density and (b) local compressibility in one direction across the center of the trap. We compare systems with the same characteristic density $\tilde{\rho} = 35$ but different trapping potentials and fillings of $V/t = 0.025$, $N_b = 1400$ and $V/t = 0.04$, $N_b = 875$. Horizontal lines show the results for homogeneous systems with $n = 1$ and the same values of $U/t$ and $\beta = 18$ as in the trap.
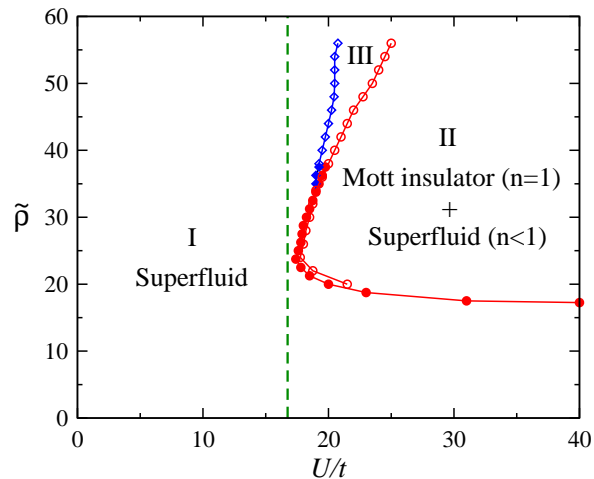
FIG. 6: (Color online) State diagram for bosons in a two-dimensional lattice in a harmonic confining potential. The boundaries between states were determined using two different traps, with $V/t = 0.025$ (filled symbols) and $V/t = 0.04$ (open symbols). Both traps lead to very similar results except for some small differences at the lowest characteristic densities. The states are: (I) a pure superfluid phase [Figs. 3(a)–3(c)], (II) a Mott insulating phase at the center of the trap surrounded by a superfluid phase with $n < 1$ [Figs. 3(d)–3(f) and Figs. 4(a)–4(c)], (III) a superfluid phase with $n > 1$ at the center of the trap surrounded by a Mott insulating phase with $n = 1$, and an outermost superfluid phase with $n < 1$ [Figs. 4(d)-4(f)]. The vertical dashed line signals the critical value of $U/t$ for the formation of the Mott insulator with $n = 1$ in the homogeneous case [15]. The inverse temperature in the trapped systems is $\beta = 18$.

homogeneous case before $\kappa$ did, usually by a difference $\delta(U/t) \sim 0.5$. In those cases, the value of $U/t$ reported at the state boundary is the average between the one obtained by $\Delta$ and the one obtained by $\kappa$. Note that this discrepancy represents, at worst, an uncertainty in the boundary of only a few percent.

Figure 6 is the central result of this paper: the state diagram for lattice bosons in a two-dimensional lattice under the influence of a harmonic trap. The different states depicted represent the following. (I) Only a superfluid phase is present in the trap, the situation in Figs. 3(a)–3(c). (Notice that in this state the density at the center of the trap can take arbitrarily high values.) (II) A Mott insulating phase at the center of the trap is surrounded by a superfluid phase with $n < 1$. Examples of this state are given in Figs. 3(d)–3(f) and Figs. 4(a)-4(c). (III) A local superfluid phase with $n > 1$ is present at the center of the trap. This phase is surrounded by a Mott insulating domain with $n = 1$, inside a superfluid phase with $n < 1$. An example of that state can be found in the right panel of Fig. 4(d)–4(f).

An important feature of the state diagram of Fig. 6 is that except for a small window of characteristic densities ($\tilde{\rho} \sim 23$), where the critical value of $U/t$ for the formation of the Mott insulating domain at the center of the trap $(U/t)_c^t$ is very close to the value in homo-geneous systems $(U/t)_c$, for most characteristic densities $(U/t)_c^t$ departs significantly from $(U/t)_c$; i.e., this state boundary depends strongly on $\tilde{\rho}$. At least for fermions [38], this is the state boundary that currently can be accurately determined experimentally. This is because the total double occupancy, which is a good indicator for distinguishing states with a Mott insulator at the center of the trap from states with higher density [29], can be accurately measured in such systems [38]. Similar measurements in bosonic systems, which have site occupancy higher than two, could allow experimentalists to reproduce our results over an even broader range of the state diagram.

The other state boundary of interest is the one between states I and III. This boundary, on the other hand, does not depend strongly on the characteristic density [39]. This means that by experimentally measuring the boundary between states I and III, which is sensitive to transport and coherence probes, one would obtain a critical value of $U/t$ for the formation of the Mott insulator that is close to the one in the homogeneous system.

To conclude, we should add that with increasing characteristic density new states with Mott insulating domains with $n > 1$ appear in the trap. Those states will form for larger values of the in-site repulsive interaction, and will be more difficult to detect experimentally.

### D.   Comparison with NIST experimental results

As mentioned in Sec. I, recent experiments have achieved the superfluid-to-Mott-insulator transition in two dimensions [3]. Here we provide a quantitative comparison with our state diagram.

We use the precise values of the curvature $V$ generated by the optical and magnetic traps, and interaction and tunneling energies $U$ and $t$ (computed using a band structure calculation) appropriate to the NIST experiments [40]. The final parameter of interest is the filling. The NIST experiments employed an array of about 70 independent 2D systems of different filling. The number of particles reported for the central 2D slice (the one with maximal filling) [3] was $N_b \approx 3000$, while the average was $N_b \approx 2000$.

Figure 7 shows the trajectories of systems with different fillings, and the NIST trapping and energy parameters, in the QMC state diagram. We have also plotted the experimentally reported critical values of $U/t$ for the formation of the Mott insulator obtained using the condensate fraction and the FWHM of the momentum distribution function. For intermediate fillings ($N_b$ between 1000 and 2000 particles) corresponding to the average filling of the array of 2D layers, the experimental results intercept (within their error bars) the QMC boundary between states I and II. The error bars reported in the experiments arise mainly from the uncertainty in the lattice depth, which translates into around a $\pm 10\%$ uncertainty in the ratio $U/t$. For the largest fillings of the 2D
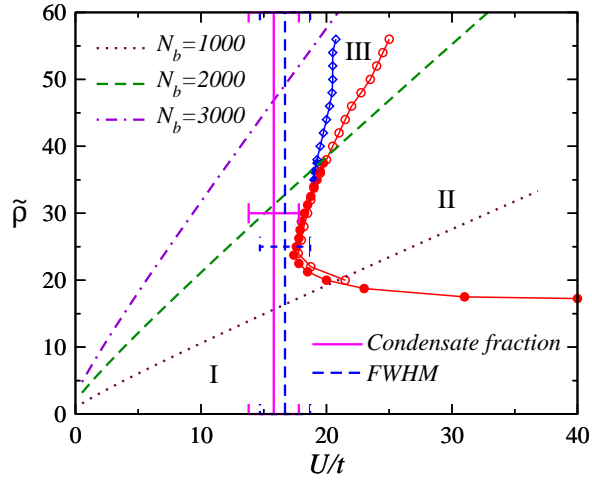
FIG. 7: (Color online) State diagram in Fig. 6 with experimental trajectories for systems with different fillings, $N_b = 1000$, 2000, and 3000. $V$, $t$, and $U$ have been chosen to correspond to the specific experiments is Ref. [3]. Vertical lines depict the critical values of $U/t$ reported in Ref. [3], computed using the condensate fraction in one case and the full width at half maximum (FWHM) of the momentum distribution function in the other [3]. The experimental errors are also plotted. The experiment and QMC give values for the critical coupling in excellent agreement.

slices ($N_b$ between 2000 and 3000 particles), we find that the experimentally reported critical values are very close to the boundary between states I and III.

Overall, the agreement between our numerical calculations and the experimental results is remarkable. It could even be considered surprising, taking into account that in the experiments only global quantities such as the condensate fraction and the FWHM of the momentum distribution function have been measured, while our state diagram is based on the behavior of local quantities such as the variance of the density and the local compressibility. The agreement between those two approaches is a priori not guaranteed [18]. New experiments in which the filling in the 2D sections is better controlled could allow experimentalists to map the state diagram in Fig. 6. Given the presence of the trapping potential in the experiments and the fact LDA fails close to $(U/t)_c$ of the homogeneous system, we believe this is a better strategy to follow to validate experiments than trying to map the phase diagram of the homogeneous system. Recent progress on the direct imaging of the density profile will also allow further detailed comparisons with simulation.

## E. Finite temperature

In order to better compare with the experiments, it is important to understand how a small increase in the temperature affects the zero-temperature state diagram reported in this paper. By small we mean a temperature that is low compared to the value of the hopping param-

eter, so we consider here temperatures $T \leq t/2$. The effect of higher temperatures ($t < T < U$) on the Mott insulating state in trapped systems has been discussed in previous works (see, e.g., Refs. [7, 8, 9, 10]).

Our QMC simulations for two-dimensional systems with $T \leq t/2$ show that low temperatures have a small effect on the state diagram in Fig. 6. We have found that in general the state boundaries move to larger values of $U/t$, with a change of up to 4% of the ground-state value depending on the filling. This effect is particularly evident for the lowest characteristic densities. For larger characteristic densities, the ones that support state III in Fig. 6, we find the effect of low temperatures to be less important.

As an example of our results, in Fig. 8 we compare density profiles and compressibilities in confined systems with $\tilde{\rho} = 44$ at different temperatures and interaction strengths. One can see there that while density and compressibility profiles in state I are almost indistinguishable for the temperatures considered here [Figs. 8(a) and 8(b), where $U/t = 16$], the ones in state III can exhibit apparent changes when close to the boundary with state II [Figs. 8(c) and 8(d), where $U/t = 21$]. However, with just a small increment of the interaction strength so that one creates state II in the ground state [Figs. 8(e) and 8(f),
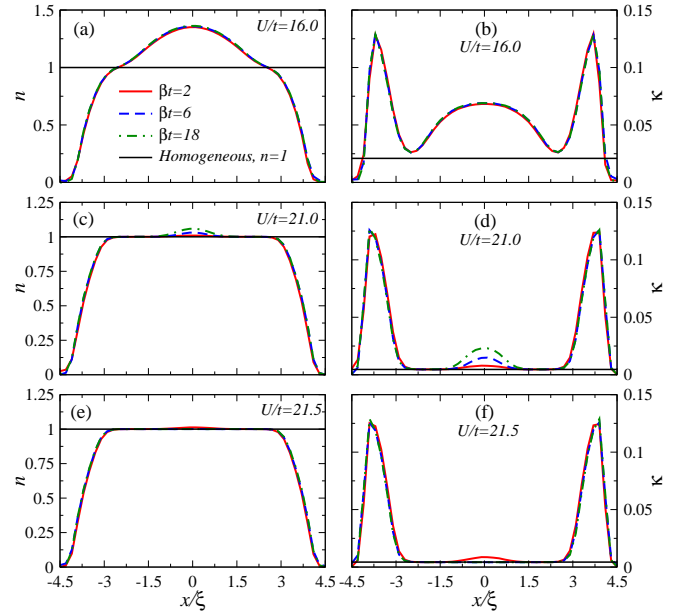


FIG. 8: (Color online) Comparison between local quantities in systems with different temperatures. We have plotted the density (left panels) and local compressibility (right panels) in one direction across the center of the trap. The ratio between the on-site repulsion and the hopping parameter is increasing from top to bottom:[(a) and (b)]$U/t = 16$, [(c) and (d)] $U/t = 21$, and [(e) and (f)] $U/t = 21.5$. All systems have the same characteristic density $\tilde{\rho} = 44$ ($N_b = 1100$, $V/t = 0.04$). Horizontal lines show the results for homogeneous systems with $n = 1$, and the same values of $U/t$ as in the trap. The differences bewteen $\kappa$ in homogeneous systems with $\beta t = 2$, 6, and 18 are indistinguishable in the figure.

where $U/t = 21.5$] the system has a full Mott insulating domain at the center of the trap for $\beta = 18$ and $\beta = 6$, while $\beta = 2$ is very close to forming one. The generic effect of the temperature can be seen to be a displacement of the state boundaries to larger values of $U/t$.

## III.  TRAPPED BOSONS IN ONE DIMENSION

In one dimension, previous work has already shown that systems with the same characteristic density $\tilde{\rho} = N_b\sqrt{V/t}$ have identical re-scaled density profiles [28], so here we will not present a detailed discussion (i.e., the $d = 1$ analogs of Figs. 3, 4, and 5 presented for $d = 2$). In addition, the behavior of the local observables defined in Sect. II is qualitatively similar to that in two-dimensional systems. Therefore, in this section, we use the same criteria to create the $d = 1$ state diagram, depicted in Fig. 9. The labeling of the states follows the same convention as in two dimensions.
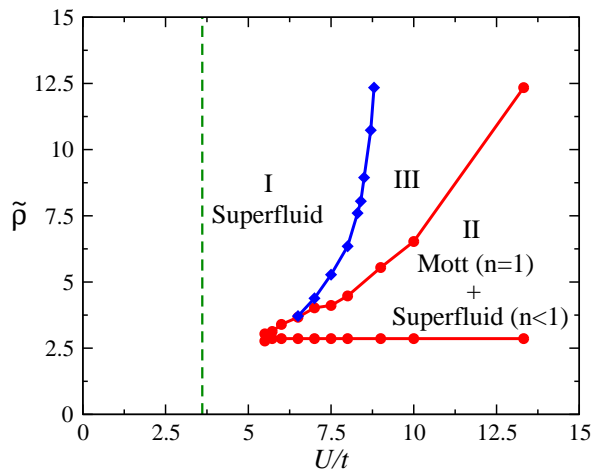
FIG. 9: (Color online) State diagram for bosons in a one-dimensional lattice with a harmonic confining potential. The state diagram was built using a trap with $V/t = 0.008$, $L = 100$, and $\beta = 10$. The states are designated in the same way as in the two-dimensional case: (I) a pure superfluid phase, (II) a Mott insulating phase at the center of the trap surrounded by a superfluid phase with $n < 1$, (III) a superfluid phase with $n > 1$ at the center of the trap surrounded by a Mott insulating phase with $n = 1$, and an outermost superfluid phase with $n < 1$. The vertical dashed line signals the critical value of $U/t$ for the formation of the Mott insulator with $n = 1$ in the homogeneous case [14].

Figure 9 shows that in one dimension the trapping potential has a more pronounced effect on displacing the critical value for the formation of the Mott insulator toward larger values of $U/t$. This can be understood if one compares the homogeneous Mott lobes in one dimension with those of higher dimensional systems, and is somehow similar to what was found in Refs. [20, 21] for the fermionic case, where, in the trap, the lowest value of $U/t$ at which a local Mott insulating phase was found
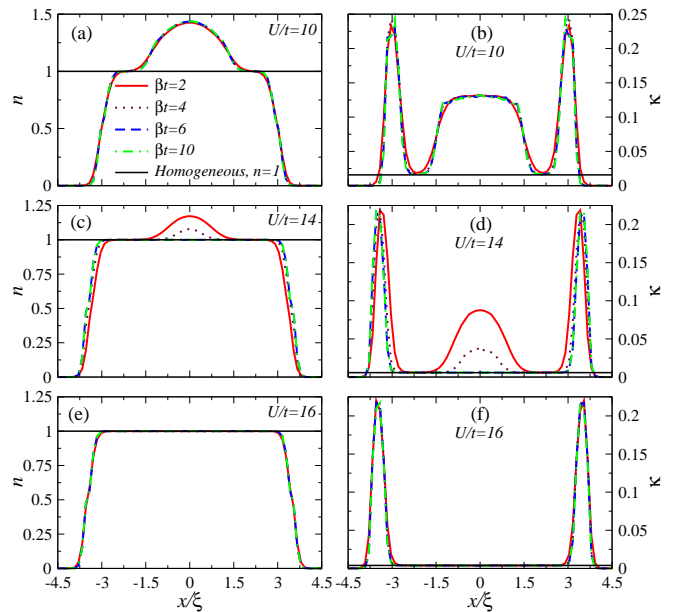
FIG. 10: (Color online) Comparison between local quantities [density (left panels) and local compressibility (right panels)] in one-dimensional systems with different temperatures. The ratio between the on-site repulsion and the hopping parameter is increasing from top to bottom: [(a) and (b)] $U/t = 10$, [(c) and (d)] $U/t = 14$, and [(e),(f)] $U/t = 16$. All systems have the same characteristic density $\tilde{\rho} = 6.96$ ($N_b = 55$, $V/t = 0.016$). Horizontal lines show the results for homogeneous systems with $n = 1$, and the same values of $U/t$ as in the trap. The differences between $\kappa$ in homogeneous systems with $\beta t = 2$, 4, 6, and 10 are indistinguishable in the figure.

was $U/t \sim 3$, to be compared with $(U/t)_c = 0$ in the homogeneous case. Another important difference between the state diagrams in two and one dimensions is that in the latter all states boundaries have a stronger dependence on the characteristic density.

In order to study the effect of finite temperatures in one-dimensional systems, we performed quantum Monte Carlo simulations using the stochastic Green's-function algorithm [41]. This algorithm allows us to compute the momentum distribution function of the bosons, a quantity that is very difficult to compute with the world-line approach.

In Fig. 10, we show examples of the effect of the temperature in one dimension. The temperature is increased up to $T = t/2$, similarly as in the two-dimensional case. Figures 10(a) and 10(b) depict a system that at zero temperature is in state III in Fig. 9. Increasing the temperature from $\beta = 10$ to $\beta = 2$ in that state does not produce large changes in the density and compressibility profiles. The region with $n \sim 1$ is the most affected by the temperature, as the Mott plateaus to the side of the central region with $n > 1$ have shrunken.

Figures 10(c) and 10(f) deal with the state that at zero temperature has a Mott insulator at the center of the trap (state II in Fig. 9). For $U/t = 14$ [Figs. 10(c) and 10(d)], one can see that increasing the temperature

beyond $\beta = 6$ melts the Mott insulator at the center of the trap, producing a central region with $n > 1$. As one increases $U/t$, $U/t = 16$ [Figs. 10(e) and 10(f)], one can see that the central Mott insulating domain survives for all temperatures analyzed here.

Overall, Fig. 10 shows that the effect of low temperatures in the state diagram in one dimension is qualitatively similar to that in two dimensions; i.e., the boundaries of state II move to larger values of $U/t$. However, our simulations show that one–dimensional systems are more affected by finite temperatures than their two-dimensional counterparts, so that any experimental comparison with our state diagram in Fig. 9 would require very low temperatures. These results also mean that the critical values for the formation of the insulator in one-dimensional trapped systems at finite temperatures are further away from the critical value in the homogeneous system at zero temperature.

To conclude, we show in Fig. 11 the effect of the temperature on the momentum distribution function of the systems with $U/t = 10$ and $U/t = 14$ in Fig. 10. (The momentum distribution function for the systems with $U/t = 16$ remains almost unchanged for the temperatures considered here.) Figure 11(a) shows that when most of the system is in a superfluid phase at zero temperature, increasing the temperature leads to a reduction in the zero-momentum peak occupation, which is a consequence of the reduction in the correlation length in the superfluid domains. On the other hand, Fig. 11(b) shows that when the ground state of the system has a very large Mott insulating domain at the center of the trap, an increase in the temperature can increase the occupation of the zero-momentum peak when the Mott insulator melts to give rise to a region with $n > 1$ at the center of the trap.
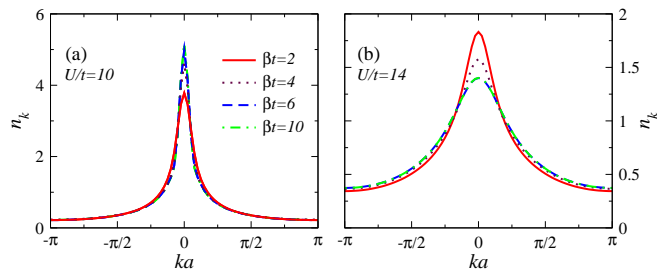


FIG. 11: (Color online) Momentum distribution function in one-dimensional systems with different temperatures. The ratio between the on-site repulsion and the hopping parameter are (a) $U/t = 10$ (at zero temperature the system is in state III), and (b) $U/t = 14$ (at zero temperature the system is in state II). All systems have the same characteristic density $\tilde{\rho} = 6.96$ ($N_b = 55$, $V/t = 0.016$).

## IV. CONCLUSIONS

In this paper we have computed the state diagrams for the formation of Mott insulating domains with $n = 1$ in lattice-boson systems confined by harmonic traps. Results have been presented in one and two dimensions and the lattice sizes considered had between 50 and 100 sites in each direction, values which are comparable to those studied by the NIST group.

We have shown that for the system sizes considered, state boundaries are accurately determined by the characteristic density, providing a state diagram for different experimental choices of trap curvature and particle number. Key features of these state diagrams are that the critical values of $U/t$ for the formation of a Mott insulator in a trap measured experimentally need not be the same as in homogeneous systems and that the LDA does not hold close to the state boundaries. We find that in two dimensions, the lowest value of $U/t$ that supports a local insulator in the trap is $U/t = 17.4$, which is approximately 4% greater than the critical value in the homogeneous case, $(U/t)_c = 16.74$. We have also shown that $(U/t)_c^T$ for the formation of the Mott insulator at the center of the trap increases with the characteristic density. These results could be verified experimentally by measuring double or higher occupancy in bosonic systems.

A comparison of our two-dimensional results with the ones of experiments at NIST shows that the particular trap, lattice depth, and particle filling used there give trajectories in the state diagram which intersect the critical coupling line near its extremal value of $U/t$. The transition point reported is in good agreement with our QMC simulations, which explicitly include the confining potential. We have also shown that, in two dimensions, finite (but low, $T \leq t/2$) temperatures have little effect on our ground-state results.

In one dimension, we find that the trapping potential has a stronger effect in moving the critical values for the formation of the Mott insulator toward larger values of $U/t$. Actually, the lowest value of $U/t$ at which we find a local Mott insulating phase in the trap (with up to 100 sites) is $U/t = 5.5$, that is, a 52% increase over the critical value in the homogeneous case, $(U/t)_c = 3.61$. We also find that state boundaries in one dimension are more sensitive to the characteristic density in the trap and to low temperatures than those in two-dimensional systems.

[1] I. Bloch, J. Dalibard, and W. Zwerger, Rev. Mod. Phys. **80**, 885 (2008).

[2] M. Greiner, O. Mandel, T. Esslinger, T. W. Hänsch, and I. Bloch, Nature (London) **415**, 39 (2002).

[3] I. B. Spielman, W. D. Phillips, and J. V. Porto, Phys. Rev. Lett. **98**, 080404 (2007); Phys. Rev. Lett. **100**, 120402 (2008).

[4] T. Stöferle, H. Moritz, C. Schori, M. Köhl, and T. Esslinger, Phys. Rev. Lett. **92**, 130403 (2004).

[5] G. G. Batrouni, V. Rousseau, R. T. Scalettar, M. Rigol, A. Muramatsu, P. J. H. Denteneer, and M. Troyer, Phys. Rev. Lett. **89**, 117203 (2002).

[6] V. A. Kashurnikov, N. V. Prokof'ev, and B. V. Svistunov, Phys. Rev. A **66**, 031601(R) (2002).

[7] B. DeMarco, C. Lannert, S. Vishveshwara, and T.-C. Wei, Phys. Rev. A **71**, 063601 (2005).

[8] G. Pupillo, C. J. Williams, and N. V. Prokof'ev, Phys. Rev. A **73**, 013408 (2006).

[9] T.-L. Ho and Q. Zhou, Phys. Rev. Lett. **99**, 120404 (2007).

[10] F. Gerbier, Phys. Rev. Lett. **99**, 120405 (2007).

[11] M. P. A. Fisher, P. B. Weichman, G. Grinstein, and D. S. Fisher, Phys. Rev. B **40**, 546 (1989).

[12] G. G. Batrouni, R. T. Scalettar, and G. T. Zimanyi, Phys. Rev. Lett. **65**, 1765 (1990).

[13] J. K. Freericks and H. Monien, Phys. Rev. B **53**, 2691 (1996).

[14] T. D. Kühner and H. Monien, Phys. Rev. B **58**, R14741 (1998).

[15] B. Capogrosso-Sansone, S. G. Söyler, N. Prokof'ev, and B. Svistunov, Phys. Rev. A **77**, 015602 (2008).

[16] D. Jaksch, C. Bruder, J. I. Cirac, C. W. Gardiner, and P. Zoller, Phys. Rev. Lett. **81**, 3108 (1998).

[17] C. Kollath, U. Schollwöck, J. von Delft, and W. Zwerger, Phys. Rev. A **69**, 031601(R) (2004).

[18] S. Wessel, F. Alet, M. Troyer, and G. G. Batrouni, Phys. Rev. A **70**, 053615 (2004).

[19] Where each state can, in general, be composed by superfluid and insulating domains with different densities.

[20] M. Rigol, A. Muramatsu, G. G. Batrouni, and R. T. Scalettar, Phys. Rev. Lett. **91**, 130403 (2003).

[21] M. Rigol and A. Muramatsu, Phys. Rev. A **69**, 053612 (2004); Opt. Commun. **243**, 33 (2004).

[22] For homogeneous systems, the Fermi-Hubbard Hamiltonian in one dimension can be exactly solved by Bethe ansatz. This, in combination with the LDA, has allowed different groups to reproduce (up to small differences at the state boundaries [23]) and extend the QMC state diagram under a harmonic confinement [24, 25, 26].

[23] G. Xianlong, M. Polini, M. P. Tosi, V. L. Campo, Jr., K. Capelle, and M. Rigol, Phys. Rev. B **73**, 165120 (2006).

[24] X.-J. Liu, P. D. Drummond, and H. Hu, Phys. Rev. Lett. **94**, 136406 (2005).

[25] V. L. Campo, Jr. and K. Capelle, Phys. Rev. A **72**, 061602(R) (2005).

[26] H. Heiselberg, Phys. Rev. A **74**, 033608 (2006).

[27] M. Rigol and A. Muramatsu, Phys. Rev. A **70**, 043627 (2004).

[28] G. G. Batrouni, H. R. Krishnamurthy, K. W. Mahmud, V. G. Rousseau, and R. T. Scalettar, Phys. Rev. A **78**, 023627 (2008).

[29] L. De Leo, C. Kollath, A. Georges, M. Ferrero, and O. Parcollet, Phys. Rev. Lett. **101**, 210403 (2008).

[30] F. Gerbier, A. Widera, S. Fölling, O. Mandel, T. Gericke, and I. Bloch, Phys. Rev. Lett. **95**, 050404 (2005).

[31] P. Sengupta, M. Rigol, G. G. Batrouni, P. J. H. Denteneer, and R. T. Scalettar, Phys. Rev. Lett. **95**, 220402 (2005).

[32] M. Rigol, R. T. Scalettar, P. Sengupta, and G. G. Batrouni, Phys. Rev. B **73**, 121103(R) (2006).

[33] C. Kollath, A. Iucci, T. Giamarchi, W. Hofstetter, and U. Schollwöck, Phys. Rev. Lett. **97**, 050402 (2006).

[34] T.-L. Dao, A. Georges, J. Dalibard, C. Salomon, and I. Carusotto, Phys. Rev. Lett. **98**, 240402 (2007).

[35] T. Roscilde, New J. Phys. **11**, 023019 (2009).

[36] D. Delande and J. Zakrzewski, Phys. Rev. Lett. **102**, 085301 (2009).

[37] J. E. Hirsch, R. L. Sugar, D. J. Scalapino, and R. Blankenbecler, Phys. Rev. B **26**, 5033 (1982).

[38] R. Jördens, N. Strohmaier, K. Günter, H. Moritz, and T. Esslinger, Nature (London) **455**, 204 (2008).

[39] In the thermodynamic limit, based on the LDA, one would expect this boundary to occur at constant $U/t$ starting from the tip in the boundary of state II.

[40] We thank J.V. Porto and I.B. Spielman for providing us with their results for these quantities.

[41] V. G. Rousseau, Phys. Rev. E **77**, 056705 (2008); Phys. Rev. E **78**, 056707 (2008).